ELSEVIER

15 August 1999

Optics Communications 167 (1999) 225–233

OPTICS COMMUNICATIONS

www.elsevier.com/locate/optcom

Full length article

# Ultrafast two-photon absorption optical thresholding of spectrally coded pulses

Z. Zheng [a,*], S. Shen [a], H. Sardesai [a,1], C.-C. Chang [a,2], J.H. Marsh [b], M.M. Karkhanehchi [b,3], A.M. Weiner [a]

[a] *School of Electrical and Computer Engineering, Purdue University, 1285 EE Building, West Lafayette, IN 47907-1285, USA*
[b] *Department of Electronics and Electrical Engineering, University of Glasgow, Glasgow, Scotland G128QQ, UK*

Received 5 February 1999; received in revised form 10 June 1999; accepted 10 June 1999

**Abstract**

We report studies on two-photon absorption (TPA) GaAs p-i-n waveguide photodetectors as optical thresholders for proposed ultrashort pulse optical code-division multiple-access (CDMA) systems. For either chirped optical pulses or spectrally phase coded pseudonoise bursts, the TPA photocurrent response reveals a strong pulseshape dependence and shows good agreement with theoretical predictions and results from conventional SHG measurements. The performance limits of the TPA optical thresholders set by the encoded bandwidth in the spectral encoding-decoding process are also discussed based on numerical simulations. Our results show the feasibility of applying such devices as nonlinear intensity discriminators in ultrahigh-speed optical network applications. 

*PACS:* 42.79.Sz; 42.50.Hz; 42.65.Re; 85.60.Gz
*Keywords:* Code division multiple access; Two-photon absorption; Optical pulse shaping; Ultrafast optics; Photodetectors; Threshold decoding

## 1. Introduction

In broadband optical networks, there are applications which require waveform analysis of ultrashort optical pulses at high speed that could be realized by all-optical signal processing techniques. For example, in the proposed coherent ultrashort pulse code-division multiple-access (CDMA) systems, multiplexing and de-multiplexing are realized by spectral phase coding of ultrashort optical pulses [1–3]. A nonlinear thresholder is needed whose output should depend on the contrast in the peak intensity of the input waveform instead of solely on the pulse energy, in order to distinguish between short optical pulses and pseudonoise bursts which result from the correct and incorrect coding-decoding process be-

* Corresponding author.
[1] Currently with Lightwave Systems Development, CIENA Corporation, 920 Elkridge Landing Road, Linthicum, MD 21090, USA.
[2] Currently with Lucent Technologies, 101 Crawfords Corner Rd., Holmdel, NJ 07733, USA.
[3] Currently with Dept. of Electronics, Faculty of Engineering, Razi University, Kermanshah, Iran.

0030-4018/99/$ - see front matter 
PII: S0030-4018(99)00313-2

tween transmitter and receiver pairs respectively. Although the nonlinear optical response would need to be very fast, the electrical response of these devices could be as slow as the data rate per channel ($\sim$ Gbit/s). Recently such a CDMA system had been demonstrated [2,3] and various optical thresholding techniques had also been proposed [4–6]. These nonlinear detectors may also be applied to the header recognition process in ultrafast time-division multiple-access (TDMA) networks, to the ultrashort pulse correlation measurements or to provide feedback signals for real-time pulseshape control [7–9].

Two-photon absorption (TPA) has drawn interest for ultrashort optical pulse measurement as a substitutive quadratic nonlinear process in place of the widely used second-harmonic generation (SHG) in phase-matched nonlinear crystals. In semiconductors, TPA is a nonresonant effect in which two photons with energies below the bandgap are absorbed simultaneously to generate a single electron-hole pair [11–13]. It becomes a significant phenomenon especially in waveguide structures and/or where ultrashort pulsed laser sources are used. Because of the higher power level and speed achieved in the state-of-the art fiber communication systems and the increasing availability of compact femtosecond laser systems, there have been intensive studies on the effect of TPA in ultrafast guided-wave nonlinear optics in recent years. Though considered as deleterious and one of the main factors in limiting all-optical switching in semiconductor waveguides [14] and leading to break-up of spatial solitons in glass waveguides [15], the nonlinear photoconductivity associated with TPA has been applied for autocorrelation measurements of ultrashort pulses [16–22,6]. Various devices have been used in these experiments, including GaAs/AlGaAs and InGaAsP waveguides [17–19], photodiodes [20], light-emitting diodes [21] and laser diodes [6]. TPA techniques have some advantages over their SHG counterpart, such as: TPA has a broader wavelength response (e.g. photon energy can vary from above half of the bandgap to close to the bandgap), while phase-matching conditions can result in a much narrower response bandwidth in the SHG process [23]; the nonlinear optical process and electrical detection process are integrated in these TPA devices, which makes these devices inherently compact and easy to use in optoelectronic systems; for waveguide structures, the increased interaction length increases the efficiency and could lead to lower power requirements.

Because of the nonlinear intensity dependence of TPA process, it had been generally assumed that the TPA process shall have some kind of pulsewidth dependence. However few thorough experimental studies on this subject had been performed, especially for pulses with complicated waveforms. Among the reports of applying TPA devices to successful correlation measurements of femtosecond pulses, there are reports of quite different pulsewidth dependence. Using the GaAs waveguide photodetector which had been demonstrated as high-sensitivity TPA autocorrelators at 1.06 $\mu$m and 1.3 $\mu$m for picosecond pulses [17], we previously studied the TPA-induced photocurrent in GaAs waveguides as a function of optical pulsewidth for unchirped subpicosecond pulses at 1.5 $\mu$m [5]. These experiments verified, for the first time to our knowledge, an inverse pulsewidth dependence of TPA on a femtosecond time scale. This result was subsequently confirmed in [20] as well. On the other hand, in other work, e.g. [21], the pulsewidth had little influence on the magnitude of TPA currents.

While these studies in [5] could show the possibility of using the nonlinear detectors in optical thresholding applications, ultrashort pulse CDMA systems [1–3] would use spectrally phase modulated optical waveforms tens of picoseconds in duration with complicated subpicosecond substructures, unlike the unchirped pulses with relatively simple pulseshapes used in previous studies. In this paper we report comprehensive experiments which investigate the dependence of TPA-induced photocurrent in GaAs waveguides on optical pulseshape not only for bandwidth limited pulses, but also for chirped and spectrally coded pulses in the subpicosecond region. We also perform comparisons between TPA and SHG experiments using shaped pulses, which, we demonstrate, are in good agreement with each other. The large contrast in the response of TPA detectors to spectrally coded vs. uncoded pulses, which is in excellent agreement with our theoretical estimations, further confirms the feasibility of using these devices as ultrafast intensity discriminators. Combined with the demonstrated subnanosecond electrical response time [5], nonlinear waveguide photodetectors could

be suitable for high speed communications using ultrashort pulses.

We note that another type of ultrafast thresholder, based on nonlinear frequency shifts in fibers, was reported in [4]. The nonlinear fiber optic thresholder realized a $>10\%$ efficiency and a 30 dB contrast ratio. The TPA thresholder achieves a weaker contrast, due to the quadratic nature of the TPA process. However, in contrast to the nonlinear fiber devices hundreds of meters in length, these semiconductor TPA devices have a much smaller latency in the detection process, which could be important in communication applications, besides their advantages of compactness.

In the following we first briefly present the theory used to describe the TPA induced photocurrent. We then describe experimental results for chirped and coded pulses with a variety of pulsewidth and compare to theory. The practical issue of effect of encoded bandwidth on the performance of the optical thresholders is also discussed based on numerical simulations.

## 2. Theoretical treatment of TPA detection of ultrashort optical pulses

Ideally, under the no-depletion condition, the average TPA photocurrent $i_{\mathrm{tpa,ave}}$ can be found as [5]:

$$i_{\mathrm{tpa,ave}} = \frac{e\Omega}{T}\int_{-T/2}^{T/2}\frac{\beta}{2h\nu}I^2\,\mathrm{d}t, \qquad (1)$$

where $I$ is the optical intensity, $\beta$ is the two-photon absorption coefficient, $T$ is the period of the mode-locked pulse stream and $\Omega$ is the volume in which carriers are generated.

As been shown in [5], for Gaussian-shape pulses of different pulsewidth, the average TPA photocurrent is given by:

$$i_{\mathrm{tpa,ave}} = e\Omega\frac{\beta T}{2\sqrt{\pi}h\nu\tau}(I_{\mathrm{ave}})^2, \qquad (2)$$

where $I_{\mathrm{ave}}$ is the average optical intensity, $\tau$ is a pulsewidth parameter and is much smaller than $T$.

According to Eq. (2), the average TPA photocurrent is proportional to the average incident optical intensity or power squared, and this power dependence can be used to experimentally prove that the TPA process is the dominant carrier generation process in the device, as in [5]. Also we see that two pulses with equal energies but very different pulsewidths (hence different peak intensities) should give different photocurrents, as the photocurrent has a $1/\tau$ dependence based on the above equation. For pulses with very complicated waveforms, this kind of pulse width dependence should still hold qualitatively; however, the simple inverse pulsewidth relation will not precisely hold unless the pulse shape is kept constant as the duration is changed. A strong contrast in photocurrent as a function of peak intensity would approximate the desired ultrafast thresholding function.

In the next section, we present our experimental studies on the pulse shape dependence of TPA photocurrents using spectrally phase modulated ultrashort optical pulses.

## 3. Experiments with chirped and spectrally coded pulses

In our experiments, a GaAs/AlGaAs ridge p-i-n waveguide detector similar to that used in [17,5] was used. In our previous studies [5], optical pulses with adjustable pulsewidths were obtained by limiting the bandwidth of pulses from a femtosecond optical parametric oscillator by filtering within a zero-dispersion double-pass pulse shaper [24]. TPA currents generated from the device clearly showed an inverse pulsewidth dependence for unchirped pulses with different bandwidths.

To further verify the feasibility of applying these waveguides as optical thresholders in CDMA systems, we have conducted studies using a short pulse fiber laser based system to generate spectrally phase modulated optical pulses. The experimental setup (see Fig. 1) utilized a part of the system that had been built as a testbed for a proposed coherent optical CDMA system [2,3]. A stretched-pulse mode-locked [25] Er-fiber ring laser generated 1.56 $\mu$m 65-fs pulses at $\sim$ 33 MHz. The laser output was passed through an interference bandpass filter, while a small portion of the unfiltered output was used as the reference beam in an SHG cross-correlator for the pulseshape measurement. Spectrally filtered pulses from the laser were amplified by a chirped pulse Er-doped fiber amplifier and then input into a fiber-pigtailed femtosecond pulse shaper. The pulse-

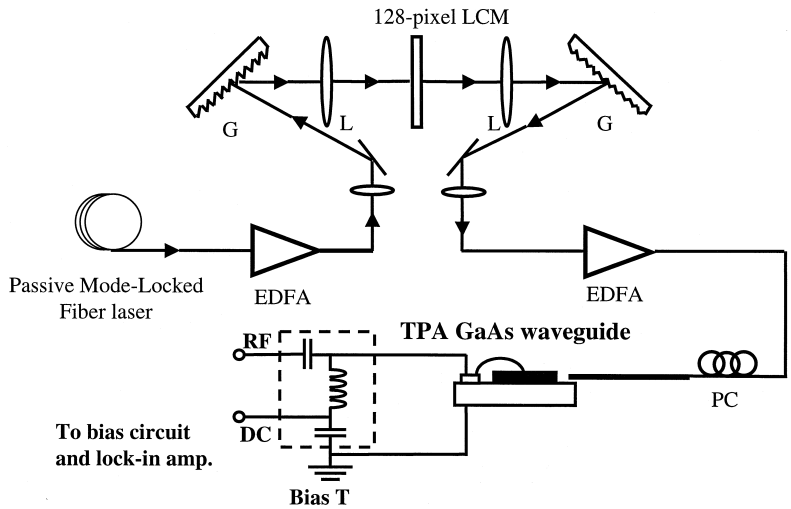


Fig. 1. Scheme of two-photon absorption thresholding experiment with coded pulses. G: 1100 line/mm grating; L: achromatic lens; LCM: liquid crystal modulator; EDFA: Er-doped fiber amplifier.

shaper consisted of a pair of 1100 lines/mm gratings and achromatic lenses (focal length = 19 cm). It was adjusted to the zero-dispersion position and had a 128-element programmable liquid crystal modulator (LCM) [10,26] in the Fourier plane. Each pixel of the LCM can be individually programmed and provide gray-scale phase modulation. The angular frequency difference between adjacent pixels is $\sim 1.1 \times 10^{11}$ rad/s. After the pulseshaper, the pulses were amplified by a second chirped pulse fiber amplifier to compensate for the loss of the pulse shaper and provide enough power for the TPA thresholder. The optical signal was then delivered to the TPA waveguide through a dispersion compensated fiber link and a fiber polarization controller (PC), which had a total length of $\sim 8$ m. The light was butt-coupled into the waveguide from single mode fiber. The coupling efficiency is expected to be lower than that obtained by focusing with a lens [5] which in turn resulted in a lower signal level compared with the previous experiments. Because of the existence of polarization dependence of TPA in this kind of waveguide photodetector [27], the state of polarization of the input beam was adjusted to excite the TE mode in the waveguide by using the PC, in order to maximize TPA signals.

In a first experiment, the LCM was used to apply a quadratic phase function to the spectrum, which in turn chirped and broadened the output pulse in the time domain. The quadratic phases applied to the ith pixel of the LCM can be described as

$$\Phi_i = \Phi_{\max} \frac{(i-64)^2}{64^2}, \tag{3}$$

where $i = 1,2,\ldots,128$; $\Phi_{\max}$ is the maximum phase shift applied. For $\Phi_{\max} > 2\pi$, the phase function is folded into the range of 0 to $2\pi$ by the relation of $\Phi_i$ modulo $2\pi$.

For these experiments the optical pulses had pulsewidth of $\sim 800$–$900$ fs immediately before being launched into the waveguide when there was only a constant phase function applied to the LCM. The pulsewidth is determined most likely by the gain narrowing effect in the EDFA and the existence of self-phase modulation leading to pulse distortion in the fiber pigtail connecting the second fiber amplifier to the TPA waveguide.

By linearly increasing the value of $\Phi_{\max}$, we could gradually increase the chirp of the pulses and the pulsewidth. Fig. 2 shows measurements of the TPA photocurrent as the pulses were broadened from $\sim 900$ fs to $\sim 2.8$ ps under a constant average power of $\sim 4.7$ mW, where $\Phi_{\max}$ was increased from 0 to $7.5\pi$. The data show that the output was nearly inversely related to the pulsewidth as measured by SHG autocorrelation for this case of chirped

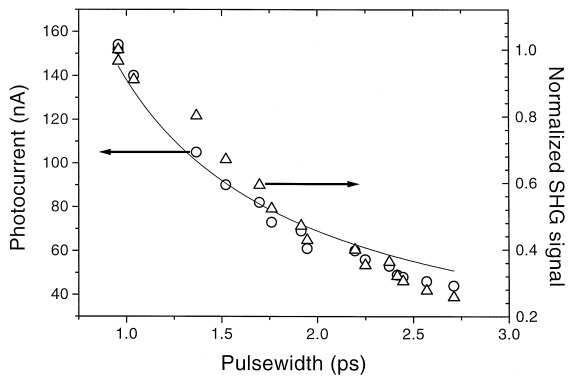


Fig. 2. Pulsewidth dependence of TPA photocurrent for chirped pulses. ∘: experimental data measured for different pulsewidths, with average input power held constant at 4.7 mW. —: $a\tau^{-1}$ curve fitted to the data. △: normalized SHG autocorrelation intensities at $\tau = 0$.

optical pulses. Also shown in Fig. 2 is the corresponding normalized variation of peak intensity (at $\tau = 0$) in SHG autocorrelation measurements. We can see a close match between the results of the TPA measurements and by conventional SHG experiments. The high sensitivity to pulsewidth shows the ability of these devices to act as peak intensity dependent detectors even for non-bandwidth limited pulses. As the pulsewidth become larger, it is observed that the current drops slightly faster than the $1/\tau$ curve. A further study on the pulse shape was performed using a cross-correlator, where the 65-fs pulses from the laser were used as reference. It was found that, as the chirp introduced in the pulse shaper increased, the pulse shape gradually deviated from the original one and had large oscillating wings or pedestals, as seen in Fig. 3, which is not described by the variation of the FWHM (full width at half maximum) pulsewidths. This could be caused by nonlinear effects in the amplifier and fiber link after the pulse shaper.

Under such conditions, the pulse shape could no longer be described by only its FWHM. However we can still predict the TPA current based on the cross-correlation measurements. Since the reference pulse was much narrower than signal pulses, we can assume, without introducing much error, that the cross-correlation traces are directly proportional to the signal pulse intensities. Using the cross-correlation data as the intensity in Eq. (1), it is possible to

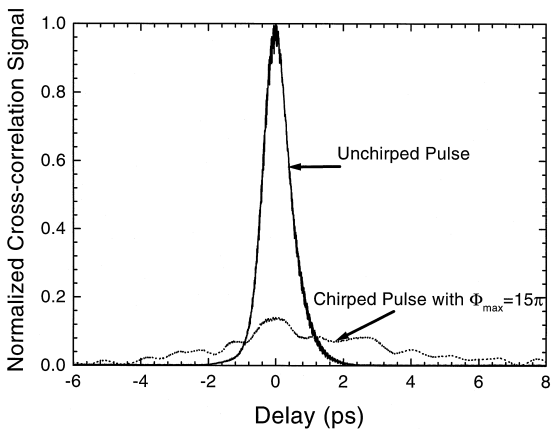


Fig. 3. Cross-correlation traces for unchirped and chirped pulses.

estimate the change in the TPA currents. TPA current and cross-correlation traces were measured for various values of $\Phi_{\max}$ ranging from $\Phi_{\max} = 0$ to $\Phi_{\max} = 15\pi$. With an initial pulsewidth of $\sim 850$ fs without spectral phase modulation applied, the pulse could be broadened to a maximum FWHM pulsewidth of $\sim 4.4$ ps. The TPA current results and the estimations based on Eq. (1) showed very good agreement over a range of $\sim 10$ times variation, as shown in Fig. 4.

While a strong pulsewidth dependence of chirped pulses could demonstrate the potential of TPA detectors as optical thresholders, the response of such devices to the spectrally coded signals as those used in the CDMA system, which have considerably more complicated pulse shapes, may be of greater rele-

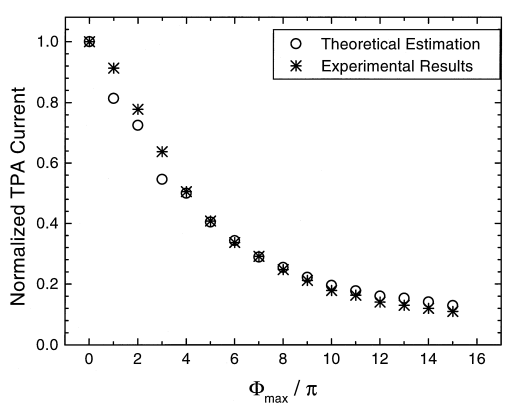


Fig. 4. Measured TPA photocurrent compared to theoretical estimation.

vance. It is well known that the performance of a CDMA system is mainly limited by the interference between different users. In the scheme described in [1], the interference shall be dominated by the non-zero response of optical thresholding devices at the receivers to incorrectly decoded signals. It can be quantitatively described by the thresholder contrast ratio, which is defined here as the ratio of the TPA current signal obtained with incorrectly decoded pulses to that obtained with correctly decoded pulses of the same pulse energy. In the proposed CDMA system, the correctly decoded pulses would be restored to the original shape with little distortion. On the other hand, incorrectly decoded pseudonoise bursts remain similar to the coded signals. Thus, in the following simulations and experiments, we approximate the contrast ratio defined above by the ratio of the TPA signal obtained with coded input pulses to that obtained with uncoded pulses. This parameter of the thresholding devices would have a significant influence on the signal-to-noise ratio and, thus, the performance of the CDMA system.

As in the CDMA system experiments [2,3], we performed experiments in which a pseudorandom M-sequence phase code was applied to the spectrum. Here, a $\pi$ phase shift is used to represent a '1' bit in the code, while a zero phase shift for a '0' bit. A length-$L$ M-sequence code is accommodated in an $N$-pixel phase mask by assigning $\lfloor N/L \rfloor$ pixels to each bit. This transformed the input pulses into low intensity pseudonoise bursts tens of picoseconds in duration. This corresponds to an encoded or incorrectly decoded signal in a CDMA system [2]. In contrast, when a constant phase is applied, the output is a bandwidth-limited short pulse, corresponding to an uncoded or correctly decoded pulse. Fig. 5a shows the SHG cross-correlations of uncoded and encoded pulses, demonstrating the dramatic change in intensity and pulsewidth. We measured the TPA photocurrents for spectra coded according to several different cyclic shifts of a length-63 M-sequence code, each of which corresponds to a new intensity and phase substructure under a similar broad envelope (two examples are shown in Fig. 5b). As shown in Fig. 6, we observed an $\sim 20$ times drop in the TPA signal compared with the responses from uncoded pulses at the same average power level for all the shifts we applied. We also estimated the contrast

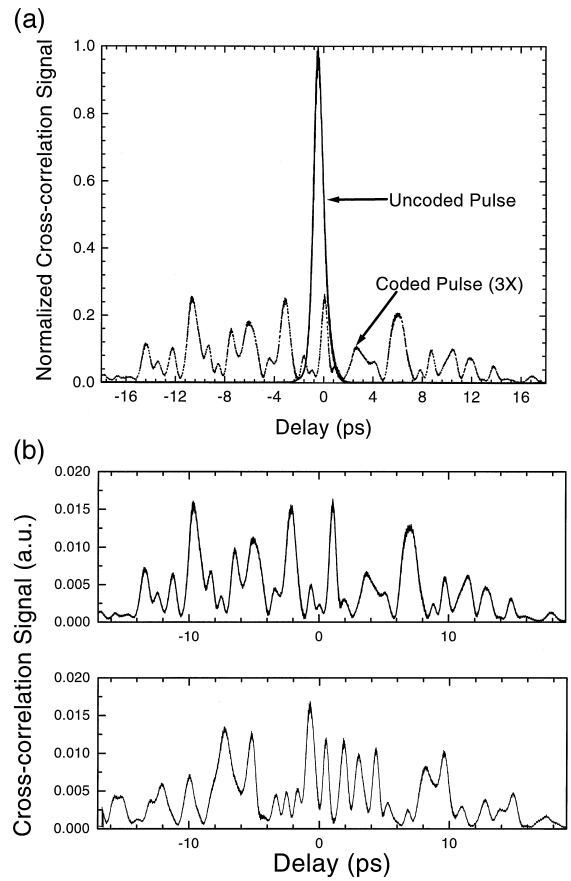


Fig. 5. (a) Cross-correlation traces for uncoded pulses and pulses coded with a pseudorandom sequence. (b) Cross-correlation traces for pulses coded with two different cyclic shifts of a pseudorandom sequence.

ratios on the basis of Eq. (1), using pulse shapes measured by SHG cross-correlation. The result plotted as theoretical contrast ratio in Fig. 6 is very close to that obtained in the TPA experiments. Once again there is excellent agreement even for these extremely complicated pulseshapes.

## 4. Limited spectral bandwidth and its influence on contrast ratios

Because of the importance of the contrast ratio in the CDMA systems, we would like to provide some further discussions on the results we obtained above.

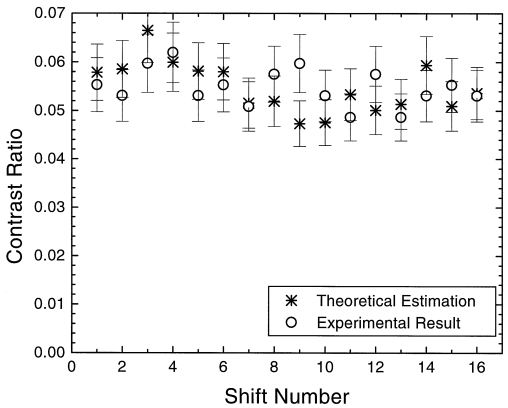


Fig. 6. Contrast ratio of TPA photocurrent and theoretical estimation based on pulseshape measurement for coded pulses.

First we see that the contrast ratio is affected by the thresholding mechanism used. For our TPA thresholders, as had been shown in [1], the maximum contrast ratio is related to $N^{-1}$ under ideal conditions, where a purely random phase code is assumed and $N$ is the code length. For a given detection mechanism, there are many other factors in the system that would affect the contrast ratio that can be realized, such as statistical properties of the code, code length and spectral shape of the input optical pulses. Here we want to specifically evaluate the limit that different spectral shapes and code lengths put on the achievable contrast ratio by numerical simulations.

To simulate the frequency coding process, where a code sequence $\{\Phi_i\}$ is applied to the input optical spectrum using a pulse shaper and a phase mask of $N$ pixels, we use the following equation to describe the output spectrum $A_{\text{out}}(\omega)$:

$$A_{\text{out}}(\omega) = A_{\text{in}}(\omega) \sum_{i=-N/2+1}^{N/2} \exp(-i\Phi_i) \times \text{rect}[i\,\delta\omega,(i+1)\,\delta\omega], \quad (4)$$

where $A_{\text{in}}(\omega)$ is the Fourier transform of the input field envelope function $E_{\text{in}}(t)$, $\delta\omega$ is the angular frequency increment between adjacent pixels, and

$$\text{rect}(x_1,x_2) = \begin{cases} 1 & x_1 \le x < x_2 \\ 0 & \text{elsewhere} \end{cases}. \quad (5)$$

For simplicity, infinite spectral resolution has been assumed, and the mask is considered as continuous with the gaps between adjacent pixels ignored. The output field envelope $E_{\text{out}}(t)$ in the time domain can be obtained from the inverse Fourier transform of $A_{\text{out}}(\omega)$.

In our experimental setup, the phase mask not only applies the spectral phase modulation to the optical spectrum but acts as an amplitude window by cutting off any spectral components out of its border, and these effects are described by the second term on the right side of Eq. (4). Therefore, the spectral coding window width is decided by the physical dimension of the mask. The input spectrum is assumed to have a Gaussian shape. For a specific spectral width, the contrast ratio is calculated based on Eq. (1) for every cyclic shift of the code. In Fig. 7, the average contrast ratio is plotted as a function of the ratio of input spectral intensity FWHM to spectral coding window width, for codes of different lengths.

For completely random phase codes, one expects a contrast ratio of $2/N$ [1]. From our simulation results using M-sequence phase codes, we also find the contrast ratio is roughly proportional to $1/N$, when the input spectrum is wider than the coding window, but with a proportionality constant reduced to the 1.3–1.6 range. The improved contrast ratio arises because pseudonoise bursts produced with M-sequence coding are smoother and less peaked than Gaussian noise bursts produced with truly random coding [24]. As the spectrum gets narrower than the window, it is equivalent to applying an additional weight function to the codes. The contrast ratio

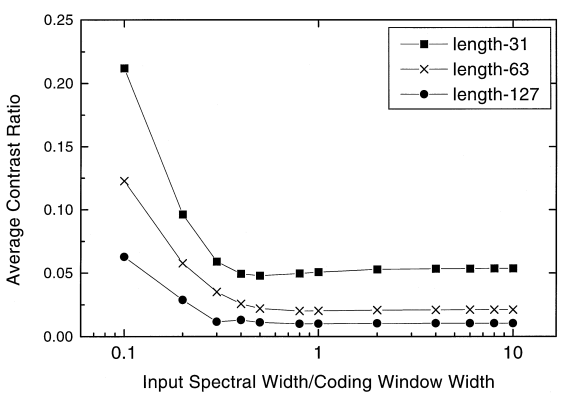


Fig. 7. Spectral width dependence of average contrast ratio for M-sequence codes of different length.

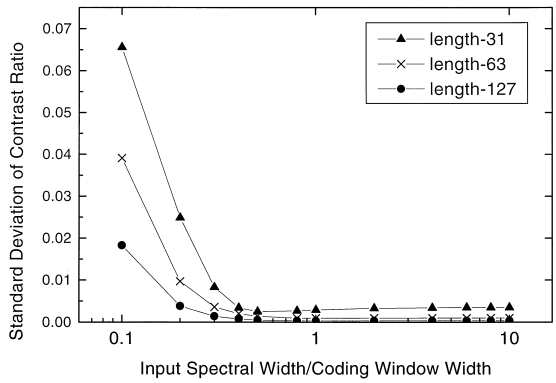


Fig. 8. Variations of contrast ratio vs. spectral width for M-sequence codes of different length.

begins to degrade significantly, because of the changed statistical properties of the codes. This is in general agreement with other studies involving a different type of optical CDMA based on spectral amplitude coding (as opposed to spectral phase coding as here) [28].

Plotted in Fig. 8 are the standard deviations of the contrast ratios for all the cyclic shifts of the M-sequence codes under various condition. It is shown that the variations in contrast ratio from one cyclic shift to another are very small for flat spectral inputs, but increase dramatically for narrower band input, which would, in turn, mean a more significant performance degradation for some users.

While it is apparently preferable to have a square-shape spectrum to be used in the encoding-decoding system, it is generally more costly to obtain broader and flatter spectrum in the system because of the constraints put on the lasers, amplifiers and other components. It is mostly likely that the spectrum used would be narrower than the spectral coding window, as in [2,3] and our results shown in this paper. Based on the results we obtained here, it is possible to use spectra with FWHMs as narrow as 40% of the coding window without too much performance degradation in the situations we discussed.

In our experiments, the power spectrum had a width of $\sim 4$ nm FWHM, and the spectral coding window was $\sim 18$ nm. This gives a ratio of 0.22. In our experiments using length-63 M-sequence codes, we observed a contrast ratio of $\sim 0.06$. This is in reasonable agreement with the simulation results in Fig. 7, considering the simplifications we had made in the simulations.

## 5. Conclusions

Our results confirm the strong intensity and pulsewidth dependence of the photocurrent from TPA waveguide photodetectors for ultrashort pulses with strong phase and amplitude modulations. For both unchirped and chirped pulses, the results correspond closely both with the theoretical predictions and with the more traditional SHG results. These experiments demonstrate the possibility of applying TPA devices as nonlinear detectors to retrieve peak intensity and pulsewidth related information at communications wavelengths and at high speed. With improved composition and structure of the waveguide, we can expect further enhancement in efficiency [19] and speed, which could reduce the power requirement and enable similar devices to be accommodated into systems with a repetition rate of $\sim 1$ Gbit/s and beyond. We can also expect the application of similar devices in ultrashort pulse detection, characterization and control systems.

## Acknowledgements

We gratefully acknowledge stimulating discussions with J.S. Aitchison. The work at Purdue University was supported by AFOSR under contract F49620-95-1-0533 and by NSF under Grant ECS-9312256 and Grant ECS-9626967.

## References

[1] J.A. Salehi, A.M. Weiner, J.P. Heritage, J. Lightwave Tech. 8 (1989) 478.
[2] C.C. Chang, H.P. Sardesai, A.M. Weiner, IEEE Photon. Technol. Lett. 10 (1998) 171.
[3] H.P. Sardesai, C.C. Chang, A.M. Weiner, J. Lightwave Tech. 16 (1998) 1953.
[4] H.P. Sardesai, A.M. Weiner, Electron. Lett. 33 (1997) 610.
[5] Z. Zheng, A.M. Weiner, J.H. Marsh, M.M. Karkhanehchi, IEEE Photon. Technol. Lett. 9 (1997) 493.
[6] L.P. Barry, B.C. Thomsen, J.M. Dudley, J.D. Harvey, Electron. Lett. 34 (1998) 358.
[7] A.M. Weiner, Prog. Quant. Electron. 19 (1995) 161.

[8] D. Meshulach, D. Yelin, Y. Silberberg, Opt. Commun. 138 (1997) 345.
[9] D. Yelin, D. Meshulach, Y. Silberberg, Opt. Lett. 22 (1997) 1793.
[10] C.C. Chang, H.P. Sardesai, A.M. Weiner, Opt. Lett. 23 (1998) 283.
[11] A. Villeneuve, C.C. Yang, G.I. Stegeman, C.N. Ironside, G.S. Celsi, R.M. Osgood, IEEE J. Quant. Electron. 30 (1994) 1172.
[12] A. Villeneuve, C.C. Yang, G.I. Stegeman, C.-H. Lin, H.-H. Lin, Appl. Phys. Lett. 62 (1993) 2465.
[13] M. Sheik-Bahae, D.C. Hutchings, D.J. Hagan, E.W. Van Stryland, IEEE J. Quant. Electron. 27 (1991) 1296.
[14] V. Mizrahi, K.W. DeLong, G.I. Stegeman, M.A. Saifi, M.J. Andrejco, Opt. Lett. 14 (1989) 1140.
[15] J.S. Aitchison, Y. Silberberg, A.M. Weiner, D.E. Leaird, M.K. Oliver, J.L. Jackel, E.M. Vogel, P.W.E. Smith, J. Opt. Soc. Am. B 8 (1991) 1290.
[16] Y. Takagi, T. Kobayashi, K. Yoshihara, S. Imamura, Opt. Lett. 17 (1992) 658.
[17] F.R. Laughton, J.H. Marsh, D.A. Barrow, E.L. Portnoi, IEEE J. Quant. Electron. 30 (1994) 838.
[18] M.M. Karkhanehchi, C.J. Hamilton, J.H. Marsh, IEEE Photon. Technol. Lett. 9 (1997) 645.
[19] H.K. Tsang, L.Y. Chan, J.B.D. Soole, H.P. LeBlanc, M.A. Koza, R. Bhat, Electron. Lett. 31 (1995) 1773.
[20] J.K. Ranka, A.L. Gaeta, A. Baltuska, M.S. Pshenichnikov, D.A. Wiersma, Opt. Lett. 22 (1997) 1344.
[21] D.T. Reid, M. Padgett, C. Mcgowan, W.E. Sleat, W. Sibbett, Opt. Lett. 22 (1997) 233.
[22] W. Rudolph, M. Sheik-Bahae, A. Bernstein, L.F. Lester, Opt. Lett. 22 (1997) 313.
[23] A.M. Weiner, IEEE J. Quant. Electron. 19 (1983) 1276.
[24] A.M. Weiner, J.P. Heritage, E.M. Kirschner, J. Opt. Soc. Am. B 5 (1988) 1563.
[25] K. Tamura, H.A. Haus, E.P. Ippen, Electron. Lett. 28 (1992) 2226.
[26] A.M. Weiner, D.E. Leaird, J.S. Patel, J.R. Wullert, IEEE J. Quant. Electron. 28 (1992) 908.
[27] M.M. Karkhanehchi, J.H. Marsh, D.C. Hutchings, Appl. Opt. 36 (1997) 7799.
[28] M. Kavehrad, D. Zaccarin, J. Lightwave Tech. 13 (1995) 534.